



1	Drought-Induced Soil Carbon Dynamics in Subtropical Forests: Emergent		
2	Divergence from Model Structures		
3			
4	Fengfeng Du ¹ , LianJun Feng ¹ , Lingyan Zhou ² , Zhizhuang Gu ³ , Yaqi Zhang ¹		
5	Zhenggang Du ^{1*} , Xuhui Zhou ¹		
6			
7			
8			
9			
10			
11	¹ Northeast Asia ecosystem Carbon sink research Center (NACC), Key Laboratory of		
12	Sustainable Forest Ecosystem Management-Ministry of Education, School of		
13	Forestry, Northeast Forestry University, Harbin, 150040, China		
14	² Shanghai Engineering Research Center of Sustainable Plant Innovation, Shanghai		
15	Botanical Garden, Shanghai, China		
16	³ Zhejiang Tiantong Forest Ecosystem National Observation and Research Station,		
17	School of Ecological and Environmental Sciences, East China Normal University,		
18	Shanghai, 200062, China		
19			
20			
21	*Corresponding author. Email: zgdu@nefu.edu.cn		
22			





ABSTRACT

23

24 Accurately quantifying drought impacts on terrestrial carbon cycling is essential for advancing predictions of climate-carbon feedbacks. However, current biogeochemical 25 models exhibit limited capability in simulating drought-induced transformations of soil 26 27 organic carbon (SOC), particularly regarding microbial processes. Here, we conducted a systematic comparative evaluation of three prevailing SOC modeling structures, 28 29 including conventional three-pool partitioning scheme (SM1), mineral and particulate-30 associated carbon partitioning scheme (SM2) and Michaelis-Menten regulated carbon-31 stabilization scheme (SM3), to elucidate their capacity in simulating soil carbon 32 dynamics under decadal drought scenarios in a subtropical forest. We found divergent effects of drought in soil C input (SM1, 66%; SM2, 10%; SM3, -4%) and mean 33 residence time (MRT; SM1, -31%; SM2, -14%; SM3, 65%), which lead to the predicted 34 SOC substantial accumulation for both SM1 and SM3 (+39.5% and +56.9%, 35 respectively) and moderate depletion (-6.1%) for SM2. The different C input directly 36 affect the passive SOC (SM1) and mineral-associated organic carbon (SM2 and SM3). 37 38 In comparison, the drought effects on passive SOC (SM1), microbe biomass (SM2) and MAOC (SM2 and SM3), lead to notable spread in MRT. These findings highlight 39 critical model structural dependencies in simulating drought-affected soil carbon 40 dynamics and emphasize the necessity for models to integrate microbial-41 physicochemical interactions for improved climate-carbon coupling projections. 42 Keywords: soil carbon stock, extreme drought, microbial enzyme activity, model 43 comparison, data assimilation, traceability analysis. 44





1 Introduction

45

46

which fundamentally alters plant-microbe-mineral interactions, serving as a key driver 47 of carbon sequestration patterns (IPCC, 2013; Han et al., 2022; Choat et al., 2018; Hao 48 49 et al., 2015). Initial drought exposure typically enhances soil organic carbon (SOC) stability via physicochemical protection mechanisms, such as reduced microbial 50 51 decomposition from moisture limitation (Schimel, 2018), increased organo-mineral 52 association due to soil contraction (Blankinship et al., 2016), and disrupted enzyme 53 diffusion (Wu et al., 2025). However, plant-derived carbon inputs decline through productivity suppression which drives by hydraulic failure (Choat et al., 2018) and 54 carbon allocation shifts away from roots (Yin et al., 2021a). Prolonged drought (e.g., >2 55 years) induces microbial adaptation strategies which may accelerate SOC loss (Barnard 56 et al., 2013; Schimel et al., 2018). The shift toward filamentous fungi dominance 57 enhances oxidative enzyme production, while necromass accumulation primes 58 destabilization of mineral-associated carbon (Liang et al., 2020; Wang et al., 2024). 59 60 However, predicting how terrestrial carbon storage responds to drought over decadal timescales remains a challenge, requiring the integration of long-term manipulative 61 experiments with models capable of capturing drought-induced changes in plant-62 microbe-mineral interactions. 63 64 In most terrestrial ecosystem models, SOC is typically represented as discrete compartments defined by their turnover times (Krinner et al., 2005; Lawrence et al., 65 2019). Early modeling approaches, such as the single-pool model proposed by Jenny et 66

Terrestrial ecosystems are facing increasing frequent stress from extreme drought





al. (1941), treated SOC as a homogeneous system. Subsequent refinements led to the 67 development of multi-pool frameworks. For example, Campbell et al. (1978) 68 categorized SOC into labile and stable organic matter. The TECO model further 69 advanced this by partitioning SOC into three pools (fast, slow, and passive SOM) with 70 71 different turnover rates (Xu et al., 2006; Du et al., 2017; Wan et al., 2025). Later developments incorporated greater complexity, such as separating recalcitrant fractions 72 73 and accounting for physically protected organic matter, which decomposes more slowly 74 than unprotected forms (Paul et al., 1978; Willard et al., 2024). Despite these 75 advancements, SOC pools remain conceptual constructs simulated via first-order kinetics. Importantly, the carbon content of individual pools cannot be empirically 76 measured, model calibration relies solely on total SOC (Guo et al., 2022). 77 Theoretical advancements in soil organic matter formation and decomposition 78 79 improve the representation of SOC in land-surface and terrestrial ecosystem models (Doelsch et al., 2020; Si et al., 2023; Cotrufo et al., 2022; Sokol et al., 2019). Measured 80 SOC fractions, such as particulate organic carbon (POC), mineral-associated organic 81 82 carbon (MAOC) and dissolved organic carbon (DOC), have been proposed to link conceptual SOC pools (Lee et al., 2020). POC is typically considered as fragments of 83 84 plant residues with a particle size > 53 µm, and it is more susceptible to external environment changes (Cotrufo et al., 2019; Benbi et al., 2014; Lugato et al., 2022). 85 MAOC generally consists of microbial and plant-derived organo-mineral complexes 86 rich in nutrients, typically < 53 μm, while also being associated with minerals and 87 embedded in soil aggregates (Si et al., 2023; Hansen et al., 2024; Villarino et al., 2021). 88





Some studies have revealed that models constrained by measurable SOC pools can 89 90 provide more accurate estimation of model parameters thereby more accurate projections of SOC dynamics (Guo et al., 2022; Tao et al., 2024; Abramoff et al., 2022). 91 Dissolved organic carbon (DOC), derived from living roots or transformed from 92 93 recalcitrant macromolecular organic matter, is approximately 2 to 3 times more efficient than litter in forming soil organic matter (Sokol et al., 2019; Cotrufo et al., 2013). 94 95 Moreover, the adsorption and desorption processes of DOC represent a key link in SOC 96 decomposition (Camino-Serrano et al., 2018; Wu et al., 2014). Consequently, 97 incorporating DOC and its interaction with SOC into models represents a crucial advance. 98 99 Soil organic matter decomposition is a stepwise process in which microbes secrete extracellular enzymes to catalyze the substrate, converting soil organic matter into 100 assimilable subunits (Caldwell et al., 2005; Ma et al., 2024; Szejgis et al., 2024). 101 Extensive manipulative experiments reveal that short-term drought limits microbial 102 activities and substrate decomposition rates by inducing osmotic stress and constraining 103 104 substrate diffusion (Honeker et al., 2024; Citerne et al., 2021). In contrast, long-term drought alters microbial community structure and carbon utilization patterns (Hueso et 105 al., 2012; Preece et al., 2019; Wang et al., 2024). As catalysts of decomposition, 106 microbial enzyme activities are impacted by drought (Sardans et al., 2010; Stursová et 107 108 al., 2012; Wu et al., 2025). For example, drought significantly reduces the activities of β-glucosidase, acid phosphatase and polyphenol oxidase, although certain oxidases 109 remain unaffected by soil moisture (Su et al., 2020a; Allison et al., 2023; Ficken et al., 110





2019). In recent years, microbial models, which focus on the process of microbial 111 decomposition, have become increasingly incorporated in process-based ecological 112 models (Moorhead et al., 2006; Lawrence et al., 2009; Allison et al., 2010; Huang et al., 113 2018). However, most microbial models focus only on simulating carbon dynamics 114 115 under warming and nitrogen deposition scenarios (Luo et al., 2020; Knorr et al., 2005; Eastman et al., 2024), while studies investigating drought effects on SOC dynamics and 116 117 microbial decomposition remain scarce. Consequently, incorporating microbial 118 enzymes to terrestrial ecosystem model are necessary to elucidate microbial regulation 119 of soil carbon responses to drought. 120 In this study, we evaluate three SOC modeling schemes with increasing complexity, including conventional three-pool partitioning scheme [SM1], mineral and particulate-121 122 associated carbon partitioning scheme [SM2] and Michaelis-Menten regulated carbon-123 stabilization scheme [SM3]. Using observational data from long-term drought experiments, we assess their validity and predictive performance. Our study addresses 124 two key questions: (1) how does decadal drought affect SOC storage in subtropical 125 126 forests? (2) do different model structures yield consistent drought impacts on SOC projections? 127

128

129

130

2 Materials and methods

2.1 Site description and data source

131 The Zhejiang Tiantong Forest Ecosystem National Field Scientific Observation and

Research Station (28°48'N, 121°47'E, 163 m a.s.l) is located in Ningbo, Zhejiang





Province. The site has a typical mid-subtropical monsoon climate with relatively 133 distinct seasons. Summers are generally mild and rainy, while winters are dry with little 134 precipitation. The annual average temperature in the study area is approximately 135 16.2 °C. The annual average precipitation and evaporation are 1384 mm and 1320 mm, 136 137 respectively, and the relative air humidity can reach 85%. The predominant soil type in the site is red-yellow soil and soil parent materials are mainly weathered products of 138 139 some granite and sedimentary rocks. The soil texture consists of sand (6.8%), silt 140 (55.5%), and clay (37.7%), with a pH ranging from about 4.4 to 5.1 (Gao et al., 2014). 141 The vegetation type in the study area is typical subtropical evergreen broad-leaved forest, with secondary forests being the main vegetation type. The forest stocking 142 density is approximately 3400 trees hm⁻². The drought experiment was established in 143 July 2013, which is composed of three experimental plots with similar terrain, 144 145 vegetation type and stand condition (Su et al., 2020b). The forcing datasets used in this study span from 2014 to 2022, including 146 photosynthetically active radiation (PAR), leaf area index (LAI), air temperature (Ta), 147 relative humidity of air (RH), soil temperature (Ts) and moisture content of soil (SWC). 148 These data were mainly measured by the station meteorological observation device. 149 The above-ground biomass data of plants were mainly estimated by allometric growth 150 equation. The C content of litter was determined by potassium dichromate oxidation 151 152 method. Soil total organic carbon and its physical and chemical properties were measured by elemental analyzer. Microbial biomass carbon was determined by 153 chloroform fumigation. DOC was determined by hot water extraction and element 154





analyzer (Zhou et al., 2013). Soil enzyme activities were determined by microplate 155 156 enzyme assay (Saiya-Cork et al., 2002; Su et al., 2020b) and was expressed by substrate conversion per gram of dry soil per hour. The soil respiration rate was measured using 157 the LI-COR 8100 portable system (LI-COR. Inc., Lincoln, NE, USA) between 9 a.m. 158 159 and 1 p.m. on 1 - 2 sunny days per month, and accumulated the data on daily scale. 2.2 Model description 160 161 All three soil models are coupled to a common vegetation submodule, which requires 162 identical environmental drivers and provides the same input data (Fig. 1). In SM1, soil 163 organic carbon is divided into three pools, including (1) a microbial pool with fast turnover; (2) a slow (chemically protected) pool, and (3) a passive (physically protected) 164 pool (Xu et al., 2006; Du et al., 2015). In SM2, SOM is divided into four pools (Si et 165 al., 2023), including (1) a dissolved organic carbon pool (DOC), which is converted 166 167 from organic matter with high molecular weight and difficult to decompose. Microbes can utilize DOC and release CO₂ (Allison et al., 2010; Lawrence et al., 2009); (2) a 168 microbial pool; (3) a particulate organic carbon pool (POC), and (4) a mineral-169 170 associated organic carbon (MAOC). SM3 is an extension of SM2 that incorporates three 171 enzyme components (β-1, 4-glucosidase (BG), polyphenol oxidase (PPO), and cellobiohydrolase (CBH)), which directly catalyze the decomposition of POC and 172 MAOC. Given that enzymes have a low carbon content and their inclusion a pool could 173 174 lead to model overparameterization, we therefore assign them a catalysis role instead of considering them as carbon pools. In these three model schemes, SM1 and SM2 175 implicitly represent microbial activities, where the decomposition of SOM governed by 176





linear, first- order dynamics. Soil C turnover times are defined by biome and poolspecific decay constants, which are modified by environmental scalars such as soil
temperature and soil moisture availability (Du et al., 2017; Du et al., 2025). In contrast,
the SM3 adopted reverse Michaelis- Menten kinetics to explicitly represent the catalytic
progress of microbial extracellular enzymes. The turnovers of DOC, POC and MAOC
are depended on the size of both the donor (substrate) and the receiver (microbial
biomass) pools. SM1 was expressed by the following equations:

$$\frac{dC_M}{dt} = I + C_S c_7 a_{67} + C_P c_8 a_{68} - C_M c_6 \tag{1}$$

$$\frac{dC_S}{dt} = I + C_M c_6 a_{76} - C_S c_7 \tag{2}$$

$$\frac{dC_P}{dt} = C_M c6a_{86} + C_S c_7 a_{87} - C_P c_8 \tag{3}$$

- Where C_M , C_S , C_P represent the C content of microbe, slow SOM and passive SOM.
- 188 I represents the C input from litters, c_6 , c_7 , c_8 represent the exit rate of C from microbes,
- slow SOM and passive SOM, and a_{67} , a_{68} , a_{76} , a_{78} represent the allocation of slow SOM
- 190 to microbes, passive SOM to microbes, microbes to slow SOM and passive SOM to
- 191 slow SOM, respectively.
- The soil C pools of SM2 were expressed as follows:

193
$$\frac{dC_{DOC}}{dt} = I + C_{POC}c_7a_{67} + C_{MAOC}c_9a_{69} - C_{DOC}c_6$$
 (4)

$$\frac{dC_{POC}}{dt} = I + C_M c_8 a_{78} - C_{POC} c_7 \tag{5}$$

$$\frac{dC_{\rm M}}{dt} = C_{\rm DOC}c_6a_{86} - C_{\rm M}c_8 \tag{6}$$

$$\frac{dC_{MAOC}}{dt} = C_{POC}c_7a_{97} + C_Mc_8a_{98} - C_{MAOC}c_9$$
 (7)





- Where C_{DOC} , C_{POC} , C_{MAOC} represent the C content of DOC, POC, MAOC.
- 198 Parameters c₆, c₇, c₈, c₉ denote the exit rate of DOC, POC, microbes and MAOC, and
- 199 a₆₇, a₆₉, a₇₈, a₈₆, a₉₇, a₉₈ represent the allocation of POC to DOC, MAOC to DOC,
- 200 microbes to POC, DOC to microbes, POC to MAOC and microbes to MAOC,
- 201 respectively.
- SM3 was expressed by the following equations:

$$\frac{dC_{DOC}}{dt} = I + a_{67}(V_{CBH.P} + V_{PPO.P} + V_{BG.P})C_{POC} + a_{69}(V_{CBH.M} + V_{PPO.M} + V_{BG.M})C_{MAOC} - \frac{V_{max.assim}C_{M}C_{DOC}}{KM_{assim} + C_{DOC}}$$
(8)

$$\frac{dC_{POC}}{dt} = I + C_M c_8 a_{78} - (V_{CBH,P} + V_{PPO,P} + V_{BG,P}) C_{POC}$$
 (9)

$$\frac{dC_{\rm M}}{dt} = C_{\rm DOC}c_6a_{86} - C_{\rm M}c_8 \tag{10}$$

$$\frac{dC_{MAOC}}{dt} = a_{97}(V_{CBH,P} + V_{PPO,P} + V_{BG,P})C_{POC} + a_{98}c_8C_M - (V_{CBH,M} + V_{PPO,M} + V_{BG,M})C_{MAOC}$$
(11)

- Where $V_{max.assim}$ and KM_{assim} denote microbe maximum assimilation rate and half-
- 208 saturation for assimilation. VCBH.P, VPPO.P, VBG.P represent catalytic rate of CBH, PPO,
- 209 BG to POC. V_{CBH.M}, V_{PPO.M}, V_{BG.M} represent catalytic rate of CBH, PPO, BG to MAOC.

$$V_{enzy.P} = \frac{V_{max.enzy} f_{enzy} C_M}{K M_{enzy} + C_{POC}}$$
 (12)

$$V_{enzy,M} = \frac{V_{max.enzy} f_{enzy} C_M}{K M_{enzy} + C_{MAOC}}$$
 (13)

- Where $V_{max.enzy}$ represent the maximum reaction rate. KM_{enzy} represent half-
- saturation for reaction, f_{enzy} represent the C ratio of CBH, PPO, BG to microbes,
- 214 respectively. The enzyme activities were calculated as following:





$$V_{enzy} = \frac{V_{max.enzy} f_{enzy} C_M C_{sub}}{K M_{enzy} + C_{sub}}$$
 (14)

Where C_{sub} denotes the C content of the enzyme-catalyzed substrate contained within a soil block with an area of 1 m² and a depth of 10 cm, and it maintains a consistent ratio of enzyme to substrate as required for experimental measurements.

We estimated model parameters using the Markov Chain Monte Carlo (MCMC) and evaluated changes in the simulated ecosystem C storage capacity using a traceability analysis framework (Supplement). The effect of drought on C storage is calculated as follows:

223
$$Drought \ Effect = \frac{\left(C_{drought} - C_{ctr}\right)}{C_{ctr}} \times 100\% \tag{15}$$

Where $C_{drought}$ represents the C content of drought, C_{ctr} represents the C content of control condition.

226

227

228

229

230

231

232

233

234

235

219

220

221

222

3.1 Model validation

3 Results

In this study, we used the Markov Chain Monte Carlo (MCMC) algorithm to constrain model parameters (Figs. 2 and S3). All three schemes incorporate 8 vegetation-related parameters (Fig. S3). SM1 included 8 soil carbon-related parameters (Fig. 2), with 5 well-constrained under control conditions (c_7 , a_{86} , a_{67} , a_{87} , a_{68}) and 5 under drought conditions (c_7 , c_8 , a_{76} , a_{86} , a_{68}). SM2 consisted 14 soil carbon-related parameters, with 7 well-constrained in the control scenario (c_9 , c_{10} , a_{74} , a_{65} , a_{67} , a_{97} , a_{78}) and 9 in the drought scenario (c_9 , c_{10} , a_{64} , a_{74} , a_{86} , a_{67} , a_{97} , a_{98} , a_{69}). SM3 had 11 well-constrained





parameters under control conditions (V_{max.assim}, V_{max.CBH}, KM_{CBH}, f_{CBH}, f_{BG}, f_{PPO}, a₆₄, a₇₄, 236 237 a75, a97, a78) and 12 under drought conditions (c6, Vmax.assim, Vmax.CBH, KMCBH, KMBG, $V_{max.PPO}$, KM_{PPO} , f_{BG} , f_{PPO} , a_{65} , a_{86} , a_{97}) in all 22 soil carbon-related parameters. 238 All three schemes calibrated by observations from the drought experimental which 239 240 had overall good agreement (Figs. S1 and S2). The simulation of vegetation C (leaf, fine root, wood) and soil respiration exhibited high accuracy. The simulated MBC by 241 242 SM1 was inferior to those simulated by SM2 and SM3, suggesting that incorporating 243 measurable C pools can improve the accuracy of MBC simulation. By comparing the 244 accuracy of POC and MAOC, we found that SM3 generally outperformed SM2, indicating that the incorporation of enzyme activities can enhance the simulation of the 245 SOC fractions, particularly with respect to MAOC. 246 3.2 Carbon simulation and prediction by three model schemes 247 248 Carbon storage from 2023 to 2100 was predicted using three different model schemes. All models consistently indicated an increasing trend in vegetation C (VegC) and a 249 decreasing trend in soil organic carbon under both control and drought conditions (Figs. 250 251 3 and S4). Specifically, under control conditions, SM1 simulated growth rates of 260% for VegC, -56.9% for SOC and 188% for total organic carbon (TOC). Under drought 252 conditions, the corresponding rates were 223%, -50.4% and 159%. SM2 projected 253 growth rates of 263% for VegC, -60.8% for SOC and 179% for TOC under control 254 255 conditions, and 217%, -55% and 151% under drought. For SM3, the simulated growth rates were 230% for VegC, -88% for SOC and 146% for TOC in the control scenario, 256 while under drought the values were 169%, -55% and 106%, respectively. 257





258 3.3 Drought effects on carbon storage 259 All three modeling schemes consistently indicated that drought reduced C content in MBC (SM1, -36.9%; SM2, -56.9%; SM3, -27.3%), VegC (SM1, -16.8%; SM2, -19.9%; 260 SM3, -25.4%) and TOC (SM1, -15%; SM2, -19.4%; SM3, -24.4%). However, the 261 262 simulated responses of SOC to drought varied among the schemes (Fig. 4). SM1 predicted an increase in SOC under drought conditions (+39.5%) compared to the 263 264 control, driving by increases in both the slow (+13%) and passive (+57%) C pools. 265 Similarly, SM3 projected a rise in SOC (+56.9%), accompanied by increases in POC 266 (+82.3%), MAOC (+88.1%), and DOC (+6.7%). In contrast, SM2 simulated a decrease in SOC (-6.1%), with reductions in DOC (-35.3%) and MAOC (-3.7%), through POC 267 increased (+43.4%). 268 By comparing the proportion of drought effects on each soil C pool simulated by 269 270 each scheme, it is apparent that different modeling schemes exhibit distinct sensitivities to drought across specific carbon pools (Fig. 4). Specifically, SM2 demonstrated greater 271 sensitivity to drought effects on microbial biomass (-54%) and DOC (-84%) compared 272 273 to SM3 (-18% and +16%, respectively). Conversely, SM3 showed higher sensitivity to drought-induced changes on POC (+82%) and MAOC (+74%) relative to SM2 (-26%) 274 and +18%, respectively). 275 3.4 Traceability analysis of drought effects 276 277 The traceability analysis revealed that both SM1 and SM3 simulated higher SOC under drought condition (SM1, 2.5 kg C m⁻²; SM3, 1.2 kg C m⁻²) compared to the control 278 (SM1, 2.1 kg C m⁻²; SM3, 0.8 kg C m⁻²) at the end of forecast period (Fig. 5). In contrast, 279





280 SM2 simulated lower SOC under drought (2.3 kg C m⁻²) compared to the control (2.5 kg C m⁻²). The increase of SOC in SM1 during drought was driven by higher soil carbon 281 input (drought, 1.0 kg C m⁻² year⁻¹; control, 0.6 kg C m⁻² year⁻¹) (Figs. 5 and 6), while 282 in SM3, it resulted from an extended soil carbon residence time (drought, 4.3 years; 283 284 control, 2.6 years). However, SM2 simulated a reduction in soil carbon residence time under drought, leading to decreased SOC. 285 286 We further analyzed the C residence times of individual pools simulated by the three 287 modeling schemes under both control and drought conditions (Fig. 6). In SM1, drought 288 increased the C residence time of passive SOM which resulted from the allocation proportions from slow SOM to passive SOM and from passive SOM to microbes were 289 elevated. For SM2, drought reduced the C residence time of microbes and increased 290 that of MAOC. The allocation proportions from POC to DOC and from DOC to 291 292 microbes were enhanced, while the allocation from MAOC to DOC declined. In SM3, drought resulted in a longer C residence time for MAOC. The allocation proportions 293 from DOC to microbes, from MAOC to DOC, and from microbes to MAOC all 294 295 increased, while the allocation from microbes to POC decreased.

296

297

298

299

300

301

4 Discussion

4.1 Response of ecosystem carbon dynamics to long-term drought

In this study, all three modeling schemes consistently indicate that drought leads to decrease in vegetable carbon (VegC), microbes carbon (Microbe C) and total organic carbon (TOC), while particulate organic carbon (POC) increases under drought

303

304

305

306

307

308

309

310

311

312

313

314

315

316

317

318

319

320

321

322

323





conditions (Figs. 3, 4 and S4). These findings are consistent with multiple fields manipulated experiments (Zhou et al., 2020; Pennisi., 2022; Schwalm et al., 2017). During drought, plants undergo physiologically adjustments and shifts in community structure in accordance with species-specific water use strategies to prevent excessive water loss (Rowland et al., 2023). These responses in turn affect C uptake via photosynthesis and C release via respiration at the ecosystem level, potentially decoupling these two processes (Meir et al., 2008). Drought consistently reduced microbial biomass carbon (MBC) across all three models, and sensitivity analysis indicated this reduction was primarily driven by increased microbial decay rates (Figs. 2 and S5). With prolonged drought duration, microbial C content exhibited a pattern of initial decline followed by a gradual recovery (Fig. 3a). Drought-induced water stress directly impairs microorganisms, leading to decreased metabolic activity (Quiroga et al., 2024). However, microorganisms can adapt to drought through physiological changes, community turnover, and evolutionary mechanisms (Martiny et al., 2015; Allison., 2023). At the community scale, droughtsensitive microbes may be replaced by more resilient taxa that immigrate into the area (Allison et al., 2008; Ricks & Yannarell., 2023). Several studies have showed that fungi exhibit greater drought adaptability compared to bacteria (Preece et al., 2019; Bastida et al., 2018; de Vries et al., 2018). Gram-positive bacteria are also better adapted to lowmoisture soils compared to Gram-negative bacteria, due to their thicker and harder cell walls, which render them less affected by drought (Castro et al., 2010; Uhlírová et al., 2005). Through in situ manipulation experiments, Bu et al (2018) and Su et al (2020b)





324 have observed shifts in microbial community structure under drought condition, which 325 may explain the gradual increase in microbial biomass under prolonged drought conditions. Besides, given that microbes directly consume DOC, the incorporation of 326 measured DOC pools in SM2 and SM3 enhances the model's ability to simulate 327 328 microbial sensitivity to drought. Simulation results from all three modeling schemes consistently showed that drought 329 330 initially decreased soil respiration, followed by a subsequently recovery (Fig. 3a). This 331 trend mirrors variations in microbial carbon content, indicating that drought regulates 332 soil respiration primarily through its control of microbial biomass (Zhao et al., 2025; Ficken & Warren., 2019). Sensitive analysis further revealed a strong positive 333 correlation between the C content of POC and the allocation proportion of litters to 334 POC (Figs. 2 and S5). These results imply that drought enhance both the carbon content 335 336 in litter and its transfer to POC, resulting in an overall increase in POC. Furthermore, since POC are directly influenced by enzymatic catalysis, SM3's heightened sensitivity 337 to drought effects on these pools underscores the model's effectiveness in capturing 338 339 enzyme-mediated processes under drought conditions. 4.2 Divergent simulations of drought effect on SOC among three modeling 340 341 schemes A key divergence among the three modeling schemes lies in their simulation of drought 342 effects on SOC components, which is the key source of discrepancy in the projected 343 carbon storage response (Figs. 4 and 6). SM1 divides SOC into three pools, including 344 MBC, slow SOM, and passive SOM. However, since only total SOC data are available 345

347

348

349

350

351

352

353

354

355

356

357

358

359

360

361

362

363

364

365

366

367





to constrain the model, the predictions of this scheme are highly sensitive to the quality and the duration of SOC observations (Fig. S5). Given the non-linear response of ecosystems to drought duration (Müller et al., 2022; Anderegg et al., 2020; Schwalm et al., 2017), models constrained by short-term observation data may introduce substantial deviation in long-term projections. In contrast, SM2 partitions the SOC into four observable carbon pools (i.e., Microbes, POC, MAOC and DOC), each independently constrained by corresponding measurements. The trajectory of SOC is thus jointly determined by these four fractions, leading to pronounced differences between the predictions of SM1 and SM2. Since both models use the same SOC data, this demonstrates the profound influence of carbon partitioning strategies on model predictions. Furthermore, drought causes the carbon input rates and carbon loss rates of individual carbon pools in SM2 deviate from the overall SOC change rate. These poolspecific discrepancies cause the SOC predictions to diverge increasingly over time between models with different structures. Differences between SM2 and SM3 are mainly reflected in the dynamics of DOC and MAOC. SM2 employs first-order linear kinetics to describe the decomposition of DOC and MAOC, where the decomposition rate is proportional to their C content. In contrast, SM3 utilizes reverse Michaelis-Menten kinetics, indicates that the decomposition of SOC is not only dependent on C content but also on microbial C and enzyme activities (Chandel et al., 2023). Under drought condition, SM2 simulates a decrease in DOC, while SM3 predicts an increase (Fig. 4). Some studies report that drought can reduce DOC concentrations (Tiwari et al., 2022; Wu et al., 2023), whereas

369

370

371

372

373

374

375

376

377

378

379

380

381

382

383

384

385

386

387

388

389





others suggest it may increase DOC due to the influence of factors such as air temperature, soil temperature, humidity, precipitation, pH, and sulfate concentrations (Evans et al., 2005; Sowerby et al., 2010). Sensitivity analysis reveals that DOC in SM2 is influenced mainly by the transfer ratio of POC to DOC and the transfer ratio of metabolic litter to DOC (Fig. S5). However, DOC dynamics are primarily controlled by the microbe maximum assimilation rate and half-saturation for assimilation in SM3, indicating that SM3 captures direct microbial regulation of DOC decomposition. Similarly, while SM2 simulates a slight decrease in MAOC under drought, SM3 predicts an increase (Fig. 4). This discrepancy stems the fact that SM3 explicitly incorporates the catalytic effects of three enzyme activities - BG, PPO and CBH - on MAOC decomposition. Drought reduces microbial enzyme activities (Figs. S1 and S2) (Bach et al., 2016; Waldrop et al., 2006), thereby weakening MAOC decomposition capacity and accumulating MAOC under drought condition. Moreover, the explicit inclusion of enzyme-mediated processes significantly improves the accuracy of POC and MAOC simulations, suggesting the importance of representing enzyme activities in SOC decomposition models. Our study enhances the understanding how drought affects forest C dynamic across different model schemes. Nevertheless, we acknowledge that several uncertainties involved in our analysis. First, we only considered three enzymes that directly catalyze soil carbon decomposition, while other enzymes (e.g., Acid phosphatase, N-acetylglycosaminidase, Peroxidase) may also contribute indirectly to this process (Su et al., 2020b). Second, when calculating enzyme activities, we applied laboratory-derived





proportional relationships between enzyme quantity and substrate quantity to field conditions, which assumes substrate availability far exceeds enzyme availability in field soils. Finally, laboratory enzyme activities measurements typically use specific substrates, whereas field soils contain multiple potential substrates that could be catalyzed, which introduces additional uncertainty in our simulations.

5 Conclusions

Accurately simulating the impacts of drought on soil carbon dynamics is of critical importance for terrestrial carbon sequestration. In this study, we integrated data assimilation and traceability analysis, devising three soil carbon decomposition schemes and exploring how different soil carbon decomposition models simulate soil carbon responses to drought. Our results revealed significant disparities in the drought effects on soil organic carbon as simulated by the three models, with these differences primarily driven by carbon input and carbon residence times of different carbon pools. Explicitly incorporating microbial enzyme activities notably altered the impacts of drought on mineral-associated organic carbon and dissolved organic carbon. These findings underscore the significant role of different carbon pool partitioning schemes, their constrainability, and the consideration of microbial enzyme catalytic processes in simulating the response of soil carbon to drought, enhancing our understanding of the complexity underlying drought effects on soil organic carbon decomposition.





411 **Acknowledgments:** This research was financially supported by the National Natural 412 Science Foundation of China (Grant No. 32241032, 31930072, 32471683, 32071593) 413 and the Fundamental Research Funds for the Central Universities (Grant No. 414 2572022BA08); Heilongjiang Touyan Innovation Team Program (Forest Carbon Sink 415 416 Assessment and Carbon Sequestration Management Innovation Team). 417 CRediT author contribution statement: F.D and Z.D. collected and analyzed the data and wrote the manuscript. Z.D. conceived, designed, and oversaw the study. F.D., L.F., 418 and Z.G. conducted the statistical analysis. F.D., X.Z., and Z.D. discussed, wrote, and 419 revised the manuscript with major contributions from L.Z. Y.Z. and G.Z. commented 420 421 on the manuscript. COMPETING INTEREST DECLARATION: Authors declare that they have no 422 competing interests. 423 DATA AND MATERIALS AVAILABILITY: Data will be made available on 424 request. 425 426





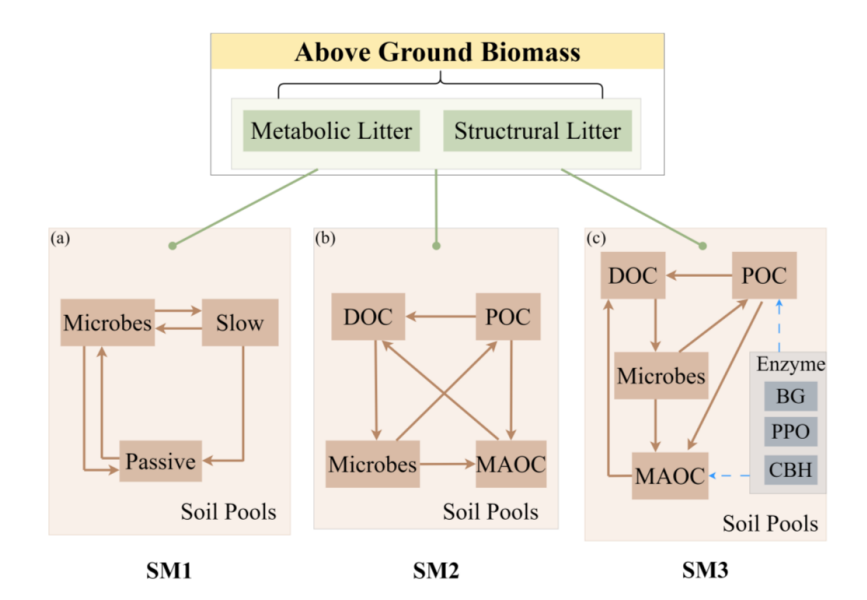


Figure 1. Conceptual diagram of the soil biogeochemical models with three schemes. **(a)** conventional three-pool partitioning scheme (SM1), **(b)** mineral and particulate-associated carbon partitioning scheme (SM2), and **(c)** Michaelis-Menten regulated carbon-stabilization scheme (SM3). All pools (boxes) and fluxes (arrows) represent C

433 ргосеss. BG, $\,\beta$ -1, 4-glucosidase, PPO, polyphenol oxidase, CBH, cellobiohydrolase.

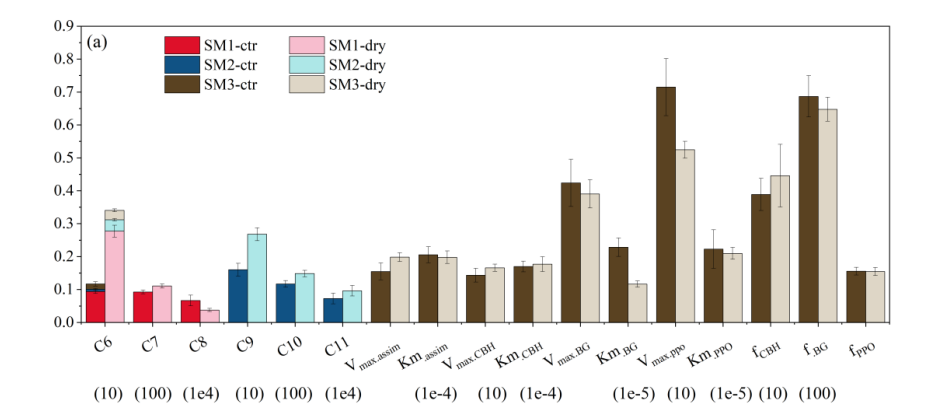
434

428 429

430







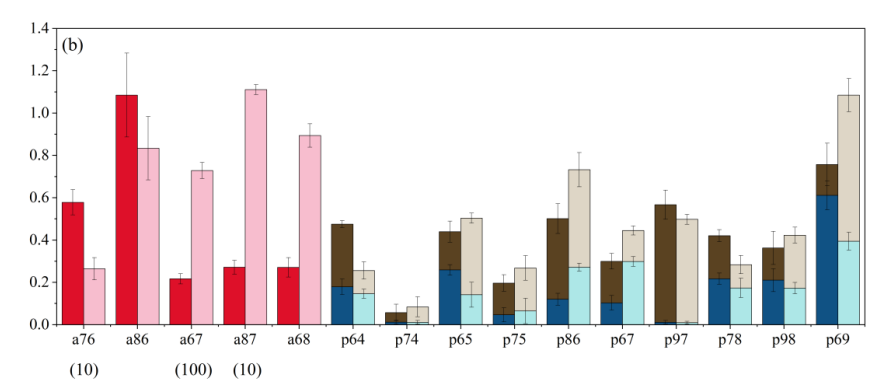


Figure 2. Maximum likelihood value (MLEs) (or means for unconstrained parameters) of the target parameters in both control and drought treatments among the three schemes. Error bars represent standard deviations (SDs). See Table S1 for parameter abbreviations and units.

443 444

445 446



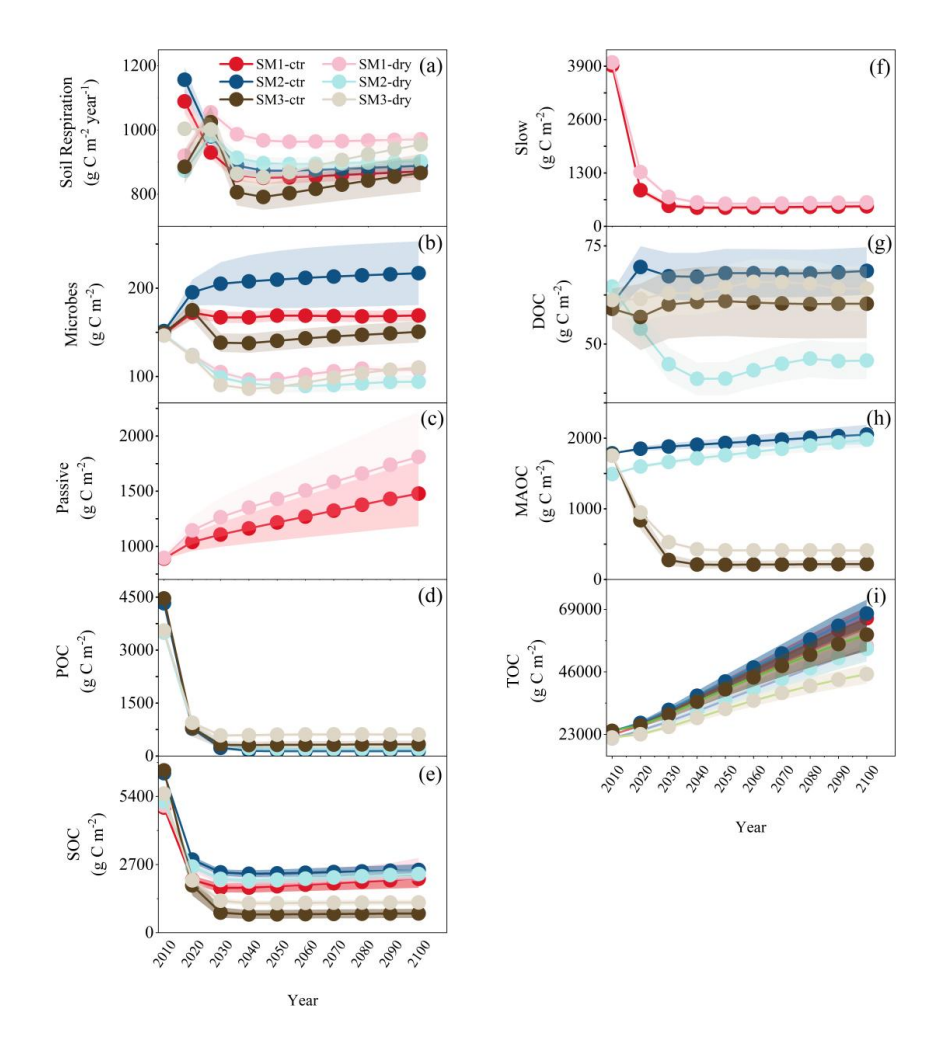


Figure 3. Predicted soil respiration (a), microbial C (b), passive SOM (c), POC (d), SOC (e), slow SOM (f), DOC (g), MAOC (h), total organic C (i) from 2014 – 2100 under dry and control conditions for three schemes.





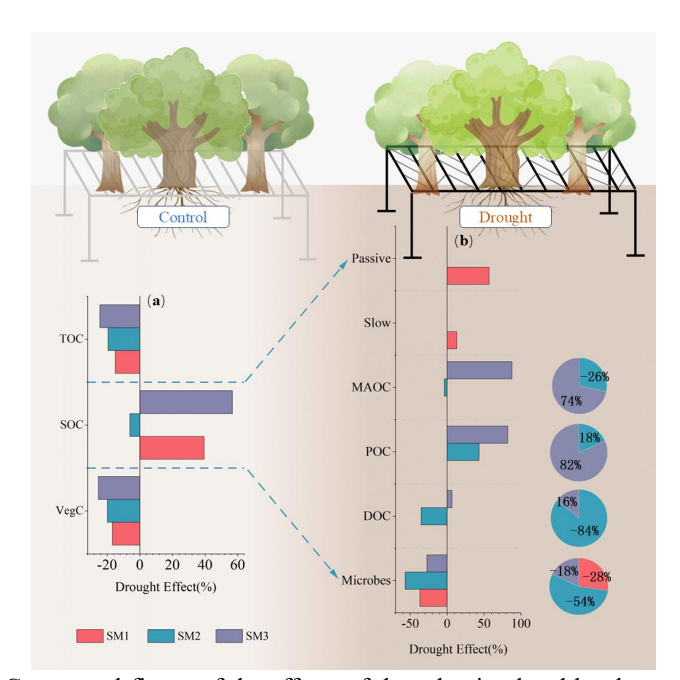


Figure 4. Conceptual figure of the effects of drought simulated by three schemes on carbon stocks. The histogram represents the drought effects on carbon pools (percentage change of the carbon pools from 2022 to 2100), and corresponding pie charts represent the proportion of the drought effects simulated by each of the three schemes for the same carbon pool, relative to the sum of the drought effects from all three schemes. TOC, soil total organic carbon. VegC, vegetation carbon.





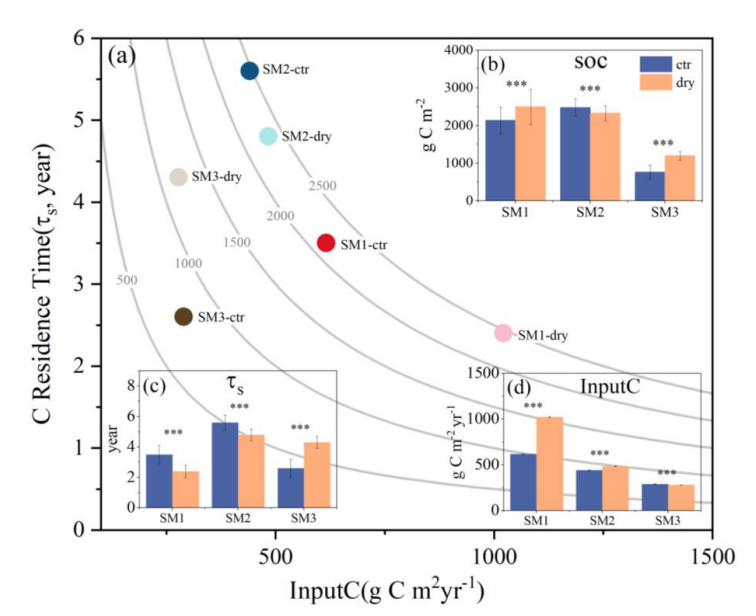


Figure 5. Predicted soil C storage capacity in 2100 by C influx (InputC, x axis) and soil carbon residence time (τ_s , y axis) between control and drought treatments in three model schemes. ***, represents p < 0.01.





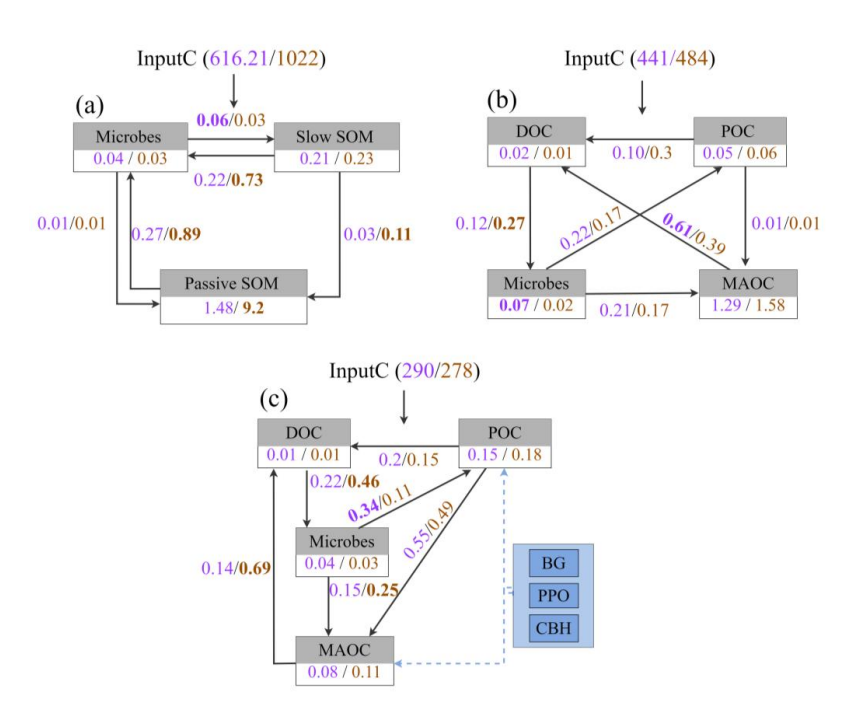


Figure 6. The carbon residence time of each soil carbon pool in the drought and control conditions simulated by three schemes and the allocative proportion of carbon turnover among some pools. The numbers in the box represents the carbon residence time, and the carbon near the arrow represents the carbon allocation proportion. Purple represents the control and brown represents the drought.





471 Appendix

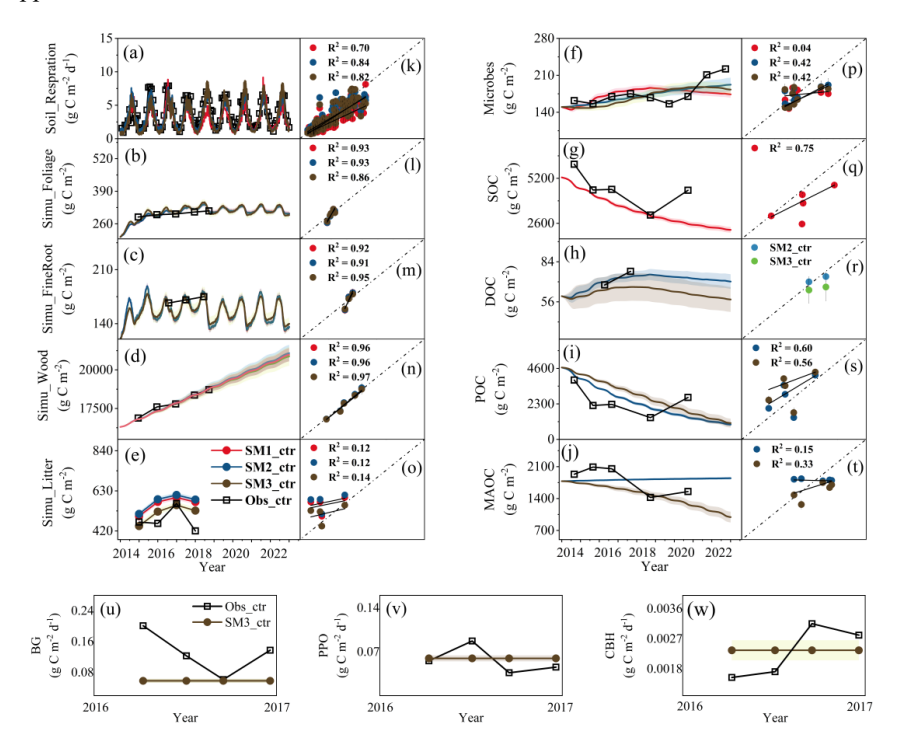


Figure A1. Comparison of the measured values (black squares) and simulated values (lines) in the control conditions of three schemes from 2014 to 2022, p < 0.05.

472 473 474

477

478





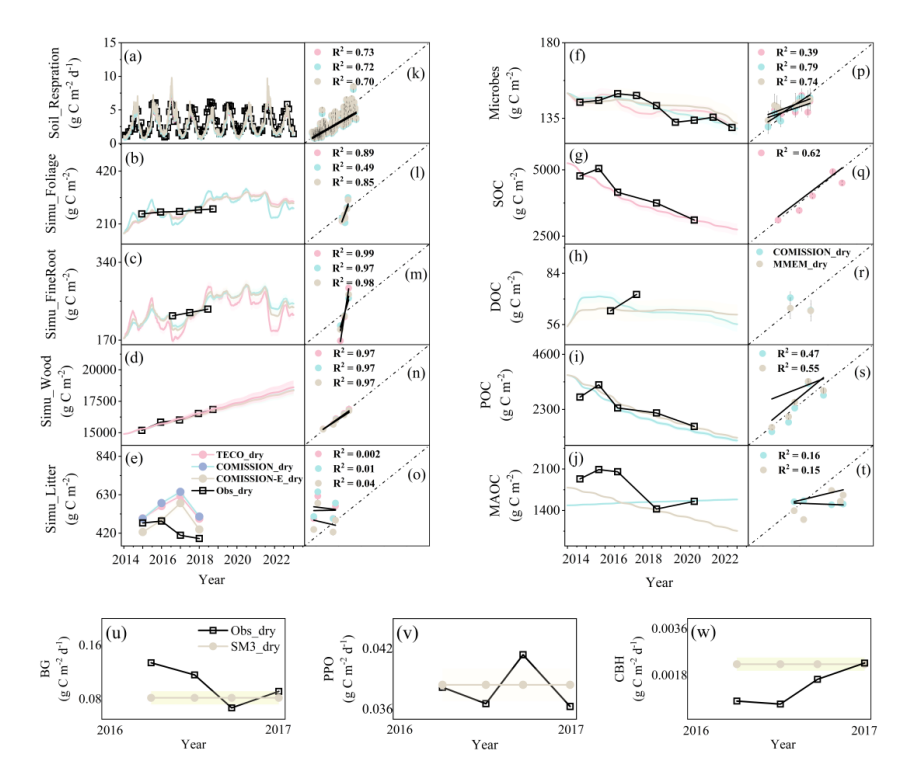


Figure A2. Comparison of the measured values (black squares) and simulated values (lines) in the drought conditions of three schemes from 2014 to 2022, p < 0.05.





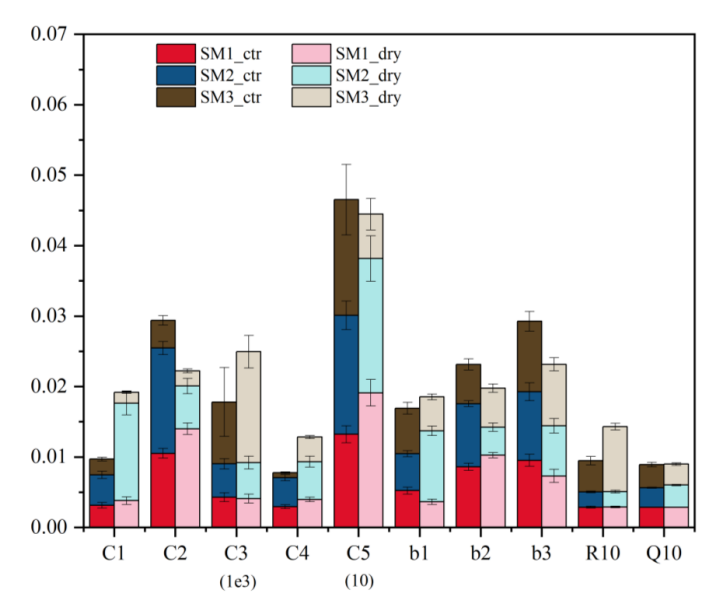


Figure A3. Maximum likelihood value (MLEs) (or means for unconstrained parameters) of the target parameters of vegetations in various models and treatments. Error bars represent standard deviations (SDs). See Table S1 for parameter abbreviations and units.

482





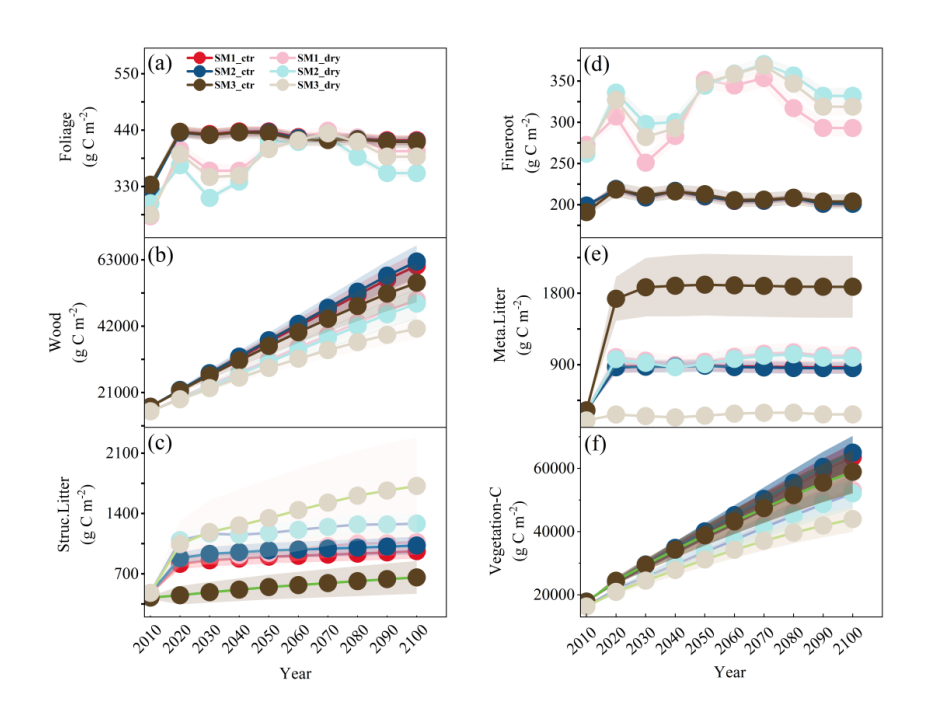


Figure A4. Predicted foliage (a), wood (b), structural litter (c), fineroot (d), Metabolic litter (e), Vegetation C (f) from 2014 - 2100 under dry and control conditions for three schemes.



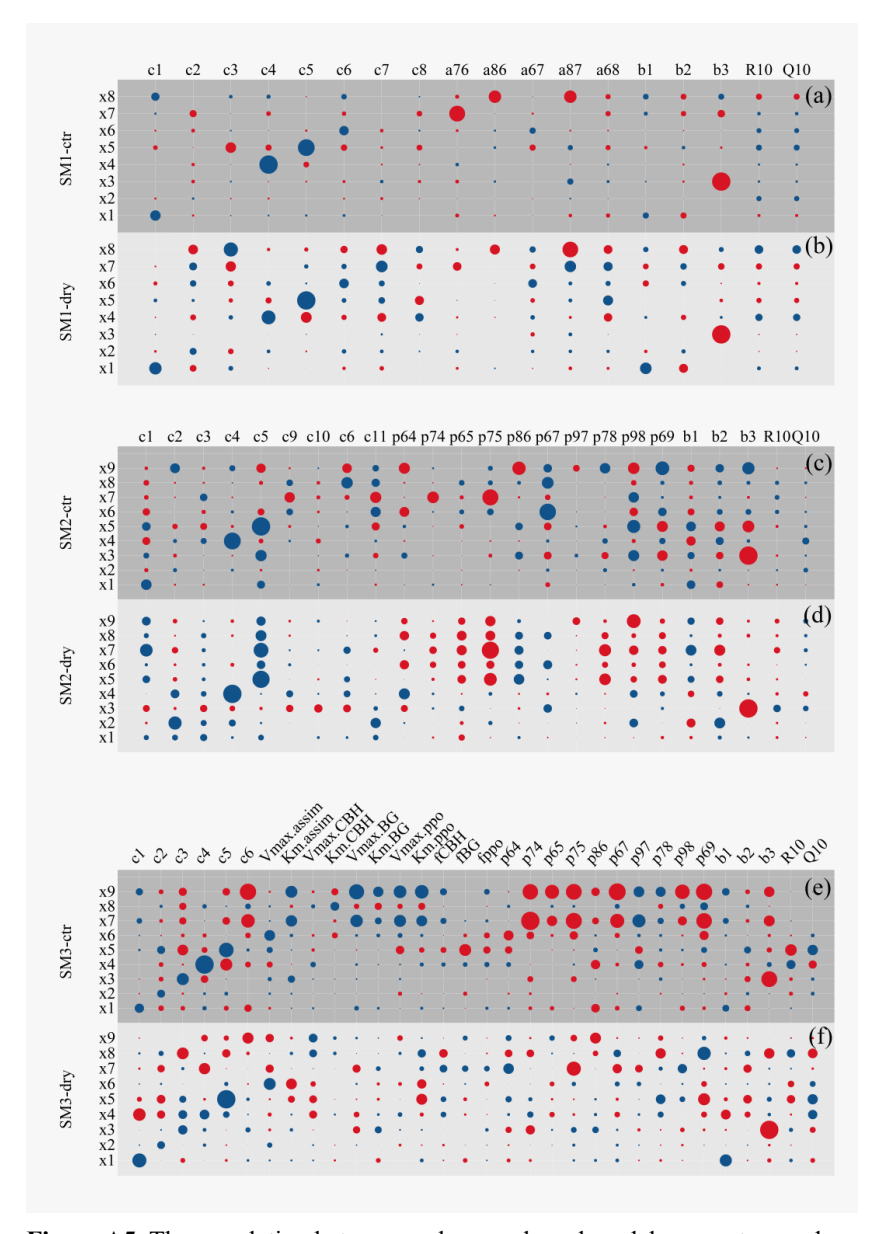


Figure A5. The correlation between carbon pools and model parameters under control and drought conditions of three schemes. Red represents positive correlation and blue represents negative correlation. The x1, x2, x3, x4, x5 represent the carbon content of foliage, fineroot, wood, metabolic litter, structural litter. x6, x7, x8 represent microbes slow SOM and passive SOM for SM1. x6, x7, x8, x9 represent DOC, POC, microbes and MAOC for SM2 and SM3.





Table A1. Target parameters of this study and their prior ranges

Parameters	Intervals	Unit	Description
CI	0.176-9.95	mg C g^{-1} d^{-1}	exit rate of C from foliage
C2	0.176-17.9	mg C g ⁻¹ d ⁻¹	exit rate of C from fineroot
C3	0.00176-0.01	mg C g^{-1} d^{-1}	exit rate of C from wood
C4	0.274-8.22	mg C g ⁻¹ d ⁻¹	exit rate of C from metabolic litter
C5	0.0548-1.64	mg C g^{-1} d^{-1}	exit rate of C from structural litter
<i>C6</i>	2.74-13.7	mg C g ⁻¹ d ⁻¹	exit rate of C from microbes
<i>C7</i>	0.027-1.37	mg C g^{-1} d^{-1}	exit rate of C from slow SOM
C8	0.00137-0.00913	mg C g^{-1} d^{-1}	exit rate of C from passive SOM
<i>C9</i>	2.74-68.5	mg C g ⁻¹ d ⁻¹	exit rate of C from DOC
C10	0.1-1	mg C g^{-1} d^{-1}	exit rate of C from POC
C11	0.00137-0.013	mg C g ⁻¹ d ⁻¹	exit rate of C from MAOC
bI	0-0.315	-	allocation of GPP to foliage
<i>b2</i>	0-0.3	-	allocation of GPP to fineroot
<i>b3</i>	0-0.3	-	allocation of GPP to wood
R10	0-1	g C m ⁻² d ⁻¹	basic respiration rate
Q10	2-5	-	temperature sensitivity of respiration
a76	0-0.5	-	allocation of microbes to slow SOM
a86	0-0.5	-	allocation of microbes to passive SOM
a67	0-0.5	-	allocation of slow SOM to microbes
a87	0-0.5	-	allocation of slow SOM to passive SOM
a68	0-1	-	allocation of passive SOM to microbes
p64	0-0.3	-	allocation of metabolic litter to DOC
p74	0-0.7	-	allocation of metabolic litter to POC
p65	0-0.6	-	allocation of structural litter to DOC
p75	0-0.4	-	allocation of structural litter to POC
p86	0-0.7	_	allocation of DOC to microbes





p67	0-0.8	-	allocation of POC to DOC
p97	0-0.2	-	allocation of POC to MAOC
p78	0-0.7	-	allocation of microbes to POC
p98	0-0.3	-	allocation of microbes to MAOC
p69	0-0.8	-	allocation of MAOC to DOC
$V_{max.assim}$	0.001-0.4	mg C mg ⁻¹ MBC d ⁻¹	microbe maximum assimilation rate
Km _{.assim}	300-3000	$\rm g \ C \ m^{-3}$	half-saturation for assimilation
$V_{max.CBH}$	0.0001-0.01	mg C mg ⁻¹ CBH d ⁻¹	maximum reaction rate of CBH
$Km_{.CBH}$	300-3000	$g C m^{-3}$	half-saturation for reaction of CBH
$V_{max.PPO}$	0.0001-0.2	mg C mg ⁻¹ PPO d ⁻¹	maximum reaction rate of PPO
$Km_{.PPO}$	300-6000	$g C m^{-3}$	half-saturation for reaction of PPO
$V_{max.BG}$	0.0001-0.2	mg C mg ⁻¹ BG d ⁻¹	maximum reaction rate of BG
$Km_{.BG}$	300-3000	$g C m^{-3}$	half-saturation for reaction of BG
f_{CBH}	0-0.01	-	CBH-to-microbial carbon ratio
f_{PPO}	0-0.2	-	PPO-to-microbial carbon ratio
f_{BG}	0-0.1	-	BG-to-microbial carbon ratio





References

- Abramoff, R. Z., Guenet, B., Zhang, H. C., Georgiou, K., Xu, X. F., Rossel, R. A. V., Yuan, W. P., and Ciais, P.: Improved global-scale predictions of soil carbon stocks with Millennial Version 2, Soil Biol Biochem., 164, https://doi.org/10.1016/j.soilbio.2021.108466, 2022.
- Anderegg, WRL., Trugman, AT., Badgley, G., Konings, AG., and Shaw, J.: Divergent forests sensitivity to repeated extreme droughts, Nat. Clim. Change., 10(12), 1091-U19, https://doi.org/10.1038/s41558-020-00919-1, 2020.
- Allison, S. D.: Microbial drought resistance may destabilize soil carbon, Trends Microbiol., 31(8), 780-787, https://doi.org/10.1016/j.tim.2023.03.002, 2023.
- Allison, S. D., and Martiny, J. B. H.: Resistance, resilience, and redundancy in microbial communities, PNAS., 105, 11512-11519, https://doi.org/10.1073/pnas.0801925105, 2008.
- Allison, S. D., Wallenstein, M. D., and Bradford, M. A.: Soil-carbon response to warming dependent on microbial physiology, Nat. Geosci., 3(5), 336-340, https://doi.org/10.1038/NGEO846, 2010.
- Basile-Doelsch, I., Balesdent, J., and Pellerin, S.: Reviews and syntheses: The mechanisms underlying carbon storage in soil, BIOGEOSCIENCES., 17(21), 5223-5242, https://doi.org/10.5194/bg-17-5223-2020, 2020.
- 522 Bastida, F., Torres, I. F., Andrés-Abellán, M., Baldrian, P., López-Mondéjar, R.,
- Vetrovsky, T., and Jehmlich, N. Differential sensitivity of total and active soil microbial communities to drought and forest management, Glob Chang Biol.., 24(1), 552-552, https://doi.org/10.1111/gcb.13953, 2018.
- Benbi, D. K., Boparai, A. K., and Brar, K.: Decomposition of particulate organic matter is more sensitive to temperature than the mineral associated organic matter, Soil Biol Biochem., 70, 183-192, https://doi.org/10.1016/j.soilbio.2013.12.032, 2014.
- Blankinship, JC., Fonte, SJ., Six, J., and Schimel, JP.: Plant versus microbial controls on soil aggregate stability in a seasonally dry ecosystem, GEODERMA., 272(39-50), https://doi.org/10.1016/j.geoderma.2016.03.008, 2016
- Barnard, RL., Osborne, CA., and Firestone, MK.: Responses of soil bacterial and fungal
 communities to extreme desiccation and rewetting, ISME J.., 7(11), 2229-2241,
 https://doi.org/10.1038/ismej.2013.104, 2013.
- 535 Bu, X. L., Gu, X. Y., Zhou, X. Q., Zhang, M. Y., Zhang, M. Y., Zhang, J., Zhou, X. H., Chen, X. Y., and Wang, X. H.: Extreme drought slightly decreased soil labile 536 organic C and N contents and altered microbial community structure in a 537 538 subtropical evergreen forest, For. Ecol. Manage., 429, https://doi.org/10.1016/j.foreco.2018.06.036, 2018. 539
- Caldwell, B. A.: Enzyme activities as a component of soil biodiversity: A review, Pedobiologia., 49(6), 637-644, https://doi.org/10.1016/j.pedobi.2005.06.003, 2005.
- Camino-Serrano, M., Guenet, B., Luyssaert, S., Ciais, P., Bastrikov, V., De Vos, B.,
 Gielen, B., Gleixner, G., Jornet-Puig, A., Kaiser, K., Kothawala, D., Lauerwald,
 R., Peñuelas, J., Schrumpf, M., Vicca, S., Vuichard, N., Walmsley, D., and





- Janssens, I. A.: ORCHIDEE-SOM: modeling soil organic carbon (SOC) and dissolved organic carbon (DOC) dynamics along vertical soil profiles in Europe, Geosci. Model Dev.., 11(3), 937-957, https://doi.org/10.5194/gmd-11-937-2018, 2018.
- Campbell, C. A.: Soil organic carbon, nitrogen, and fertility, Dev. Soil Sci.., 8, 173-271,
 https://doi.org/10.1016/S0166-2481(08)70020-5, 1978.
- Castro, H. F., Classen, A. T., Austin, E. E., Norby, R. J., and Schadt, C. W.: Soil
 Microbial Community Responses to Multiple Experimental Climate Change
 Drivers, Appl. Environ. Microbiol., 76(4), 999-1007,
 https://doi.org/10.1128/AEM.02874-09, 2010.
- Chandel, A. K., Jiang, L. F., and Luo, L. Q.: Microbial Models for Simulating Soil
 Carbon Dynamics: A Review, J GEOPHYS RES- BIOGEO., 128(8),
 https://doi.org/10.1029/2023JG007436, 2023.
- Choat, B., Brodribb, T. J., Brodersen, C. R., Duursma, R. A., López, R., and Medlyn,
 B. E.: Triggers of tree mortality under drought, NATURE., 558(7711), 531-539,
 https://doi.org/10.1038/s41586-018-0240-x, 2018.
- Ciais, P., Reichstein, M., Viovy, N., Granier, A., Ogée, J., Allard, V., Aubinet, M., 560 Buchmann, N., Bernhofer, C., Carrara, A., Chevallier, F., De Noblet, N., Friend, 561 AD., Friedlingstein, P., Grünwald, T., Heinesch, B., Keronen, P., Knohl, A., 562 Krinner, G., Loustau, D., Manca, G., Matteucci, G., Miglietta, F., Ourcival, JM., 563 Papale, D., Pilegaard, K., Rambal, S., Seufert, G., Soussana, JF., Sanz, MJ., 564 Schulze, ED., Vesala, T., and Valentini, R.: Europe-wide reduction in primary 565 566 productivity caused by the heat and drought in 2003, NATURE., 437(7058), 529-333, https://doi.org/10.1038/nature03972, 2005. 567
- Citerne, N., Wallace, H. M., Lewis, T., Reverchon, F., Omidvar, N., Hu, H. W., Shi, X.
 Z., Zhou, X. H., Zhou, G. Y., Farrar, M., Rashti, M. R., and Bai, S. H.: Effects of
 Biochar on Pulse C and N Cycling After a Short-term Drought: a Laboratory Study,
 J. Soil Sci. Plant Nutr.., 21(4), 2815-2825, https://doi.org/10.1007/s42729-021-00568-z, 2021.
- Cotrufo, M. F., and Lavallee, J. M.: Soil organic matter formation, persistence, and
 functioning: A synthesis of current understanding to inform its conservation and
 regeneration, Adv. Agron., 172, 1-66, https://doi.org/10.1016/bs.agron.2021.11.002,
 2022.
- 577 Cotrufo, M. F., Ranalli, M. G., Haddix, M. L., Six, J., and Lugato, E.: Soil carbon 578 storage informed by particulate and mineral-associated organic matter, Nat. 579 Geosci., 12(12), 989-994, https://doi.org/10.1038/s41561-019-0484-6, 2019.
- Cotrufo, M. F., Wallenstein, M. D., Boot, C. M., Denef, K., and Paul, E.: The Microbial 580 Efficiency-Matrix Stabilization (MEMS) framework integrates plant litter 581 decomposition with soil organic matter stabilization: do labile plant inputs form 582 stable soil organic matter? Glob Chang Biol... 19(4), 583 https://doi.org/10.1111/gcb.12113, 2013. 584
- Du, F. F., Zhang, Y. M., Zhou, L. Y., Dietrich, P., Zhou, G. Y., Wang, J., Zhang, Q. Z.,
 Wang, X. C., Du, Z. G., and Zhou, X. H.: Similar carbon accumulation rates with
 distinct drivers in two temperate forest restoration approaches, CATENA., 258,
 https://doi.org/10.1016/j.catena.2025.109249, 2025.





- Du, Z. G., Nie, Y. Y., He, Y. H., Yu, G. R., Wang, H. M., and Zhou, X. H.:
 Complementarity of flux- and biometric-based data to constrain parameters in a
 terrestrial carbon model, TELLUS B., 67, https://doi.org/10.3402/tellusb.v67.24102,
 2015.
- Du, Z. G., Zhou, X. H., Shao, J. J., Yu, G. R., Wang, H. M., Zhai, D. P., Xia, J. Y., and
 Luo, YQ.: Quantifying uncertainties from additional nitrogen data and processes
 in a terrestrial ecosystem model with Bayesian probabilistic inversion, Adv. Model.
 Earth Syst., 9(1), 548-565, https://doi.org/10.1002/2016MS000687, 2017.
- Eastman, B. A., Wieder, W. R., Hartman, M. D., Brzostek, E. R., Peterjohn, and W. T.
 Can models adequately reflect how long-term nitrogen enrichment alters the forest soil carbon cycle? BIOGEOSCIENCES., 21(1), 201-221, https://doi.org/10.5194/bg-21-201-2024, 2024.
- Evans, C. D., Monteith, D. T., and Cooper, D. M.: Long-term increases in surface water
 dissolved organic carbon: Observations, possible causes and environmental
 impacts, Environ. Pollut., 137(1), 55-71, https://doi.org/10.1016/j.envpol.2004.12.031,
 2005.
- Ficken, C. D., and Warren, J. M.: The carbon economy of drought: comparing respiration responses of roots, mycorrhizal fungi, and free-living microbes to an extreme dry-rewet cycle, PLANT SOIL., 435(1-2), 407-422, https://doi.org/10.1007/s11104-018-03900-2, 2019.
- Gao, Q., Hasselquist, N. J., Palmroth, S., Zheng, Z. M., and You, W. H.: Short-term
 response of soil respiration to nitrogen fertilization in a subtropical evergreen
 forest, Soil Biol Biochem., 76, 297-300, https://doi.org/10.1016/j.soilbio.2014.04.020,
 2014.
- Guo, X. W., Rossel, R. A. V., Wang, G. C., Xiao, L. J., Wang, M. M., Zhang, S., and
 Luo, Z. K.: Particulate and mineral-associated organic carbon turnover revealed
 by modelling their long-term dynamics, Soil Biol Biochem., 173,
 https://doi.org/10.1016/j.soilbio.2022.108780, 2022.
- Han, Y. A., Deng, J. J., Zhou, W. M., Wang, Q. M., and Yu, D. P.: Seasonal Responses
 of Hydraulic Function and Carbon Dynamics in Spruce Seedlings to Continuous
 Drought, Front. Plant Sci., 13, https://doi.org/10.3389/fpls.2022.868108, 2022.
- Hansen, P. M., Even, R., King, A. E., Lavallee, J., Schipanski, M., and Cotrufo, M. F.:
 Distinct, direct and climate-mediated environmental controls on global particulate
 and mineral-associated organic carbon storage, Glob Chang Biol., 30(1),
 https://doi.org/10.1111/gcb.17080, 2024.
- Hao, X. C., and Singh, V. P.: Drought characterization from a multivariate perspective:
 A review, J. Hydrol., 527, (668-678), https://doi.org/10.1016/j.jhydrol.2015.05.031, 2015.
- 2015.
 Honeker, L. K., Pugliese, G., Ingrisch, J., Fudyma, J., Gil-Loaiza, J., Carpenter, E.,
 Singer, E., Hildebrand, G., Shi, L. L., Hoyt, D. W., Chu, R. K., Toyoda, J.,
- Krechmer, J. E., Claflin, M. S., Ayala-Ortiz, C., Freire-Zapata, V., Pfannerstill, E.
- 630 Y., Daber, L. E., Meeran, K., Dippold, M. A., Kreuzwieser, J., Williams, J., Ladd,
- S. N., Werner, C., Tfaily, M. M., and Meredith, L. K.: Drought re-routes soil microbial carbon metabolism towards emission of volatile metabolites in an





- 633 artificial tropical rainforest, Nat. Microbiol.., 9(4), 1146-1147, 634 https://doi.org/10.1038/s41564-023-01507-7, 2024.
- Huang, Y., Guenet, B., Ciais, P., Janssens, I. A., Soong, J. L., Wang, Y. L., Goll, D.,
 Blagodatskaya, E., and Huang, Y. Y.: ORCHIMIC (v1.0), a microbe-mediated
 model for soil organic matter decomposition, Geosci. Model Dev., 11(6), 2111 2138, https://doi.org/10.5194/gmd-11-2111-2018, 2018.
- Hueso, S., García, C., and Hernández, T.: Severe drought conditions modify the
 microbial community structure, size and activity in amended and unamended soils,
 Soil Biol Biochem., 50(167-173), https://doi.org/10.1016/j.soilbio.2012.03.026, 2012.
- IPCC (intergovernmental Panel on Climate Change), Climate Change 2013: the
 Physical Science Basis, Cambridge University Press, Cambridge, UK, 2013.
- Jenny, H.: Factors of soil formation, McGraw-Hill, New York, 1941.
- Knorr, W., Prentice, I. C., House, J. I., and Holland, E. A.: Long-term sensitivity of soil
 carbon turnover to warming, NATURE., 433(7023), 298-301,
 https://doi.org/10.1038/nature03226, 2005.
- 648 Krinner, G., Viovy, N., de Noblet-Ducoudré, N., Ogée, J., Polcher, J., Friedlingstein, P.,
- Ciais, P., Sitch, S., and Prentice, I. C.: A dynamic global vegetation model for
 studies of the coupled atmosphere-biosphere system -: art. no. GB1015, Global
 Biogeochem. Cycles., 19(1), https://doi.org/10.1029/2003GB002199, 2005.
- Lawrence, C. R., Neff, J. C., and Schimel, J. P.: Does adding microbial mechanisms of
 decomposition improve soil organic matter models? A comparison of four models
 using data from a pulsed rewetting experiment, Soil Biol Biochem., 41(9), 1923 1934, https://doi.org/10.1016/j.soilbio.2009.06.016, 2009.
- Lawrence, D. M., Fisher, R. A., Koven, C. D., Oleson, K. W., Swenson, S. C., Bonan,
 G., Collier, N., Ghimire, B., van Kampenhout, L., Kennedy, D., Kluzek, E.,
 Lawrence, P. J., Li, F., Li, H. Y., Lombardozzi, D., Riley, W. J., Sacks, W. J., Shi,
- 659 M. J., Vertenstein, M., Wieder, W. R., Xu, C. G., Ali, A. A., Badger, A. M., Bisht,
- G., van den Broeke, M., Brunke, M. A., Burns, S. P., Buzan, J., Clark, M., Craig,
- A., Dahlin, K., Drewniak, B., Fisher, J. B., Flanner, M., Fox, A. M., Gentine, P.,
- Hoffman, F., Keppel-Aleks, G., Knox, R., Kumar, S., Lenaerts, J., Leung, L. R.,
- Lipscomb, W. H., Lu, Y. Q., Pandey, A., Pelletier, J. D., Perket, J., Randerson, J. T., Ricciuto, D. M., Sanderson, B. M., Slater, A., Subin, Z. M., Tang, J. Y., Thomas,
- R. Q., Martin, M. V., and Zeng, X. B.: The Community Land Model Version 5:
- Description of New Features, Benchmarking, and Impact of Forcing Uncertainty.
- 667 J. Adv. Model. Earth Syst, 11(12), 4245-4287. 668 https://doi.org/10.1029/2018MS001583, 2019.
- Lee, J., and Rossel, R. V. A.: Soil carbon simulation confounded by different pool initialization, Nutr. Cycling Agroecosyst., 116(2), 245-255, https://doi.org/10.1007/s10705-019-10041-0, 2020.
- Liang, C., Kästner, M., and Joergensen, R. G.: 2020. Microbial necromass on the rise:

 The growing focus on its role in soil organic matter development. Soil Biol
- 674 Biochem, 150, https://doi.org/1016/j.soilbio.2020.108000, 2020.
- 675 Luo, Z. K., Luo, Y. Q., Wang, G. C., Xia, J. Y., and Peng, C. H.: Warming-induced





- global soil carbon loss attenuated by downward carbon movement. Glob Chang Biol., 26(12), 7242-7254, https://doi.org/10.1111/gcb.15370, 2020.
- 678 Martiny, J. B. H., Jones, S. E., Lennon, J. T., and Martiny, A. C.: Microbiomes in light 679 of traits: A phylogenetic perspective, SCIENCE., 350(6261), 680 https://doi.org/10.1126/science.aac9323, 2015.
- Meir, P., Metcalfe, D. B., Costa, A. C. L., and Fisher, R. A.: The fate of assimilated
 carbon during drought: impacts on respiration in Amazon rainforests, PHILOS T
 R SOC B., 363(1498), 1849-1855, https://doi.org/10.1098/rstb.2007.0021, 2008.
- 684 Moorhead, D. L., Sinsabaugh, R. L.: A theoretical model of litter decay and microbial 685 interaction, Ecol. Monogr., 76(2), 151-174, https://doi.org/10.1890/0012-9615(2006)076[0151:ATMOLD]2.0.CO;2, 2006.
- Müller, L. M., and Bahn, M.: Drought legacies and ecosystem responses to subsequent
 drought, Glob Chang Biol., 28(17), 5086-5103. https://doi.org/10.1111/gcb.16270,
 2022.
- Paul, E. A., and Van Vee, J. A.: The use of tracers to determine the dynamic nature of organic matter, Trans. Int. Congr. Soil Sci., 11(3), 61-102, 1978.
- Pennisi, E.: Global drought experiment reveals the toll on plant growth, Science., 377(6609), 901-910, https://doi.org/10.1126/science.ade5540.Epub 2022 Aug 25, 2022.
- Preece, C., Verbruggen, E., Liu, L., Weedon, J. T., and Peñuelas, J.: Effects of past and current drought on the composition and diversity of soil microbial communities, Soil Biol Biochem., 131(28-39), https://doi.org/10.1016/j.soilbio.2018.12.022, 2019.
- 697 Quiroga, G., Castagneyrol, B., Abdala-Roberts, L., and Moreira, X.: A meta-analysis of 698 the effects of climate change-related abiotic factors on aboveground and 699 belowground plant-associated microbes, OIKOS., 2024(7), 700 https://doi.org/10.1111/oik.10411, 2024.
- Ricks, K. D., and Yannarell, A. C.: Soil moisture incidentally selects for microbes that
 facilitate locally adaptive plant response, P ROY SOC B-BIOL SCI., 290(2001),
 https://doi.org/10.1098/rspb.2023.0469, 2023.
- 704 Rowland, L., Ramírez-Valiente, J. A., Hartley, I. P., and Mencuccini, M.: How woody
- plants adjust above- and below-ground traits in response to sustained drought, New Phytol., 239(4), 1173-1189, https://doi.org/10.1111/nph.19000, 2023.
- Saiya-Cork, K. R., Sinsabaugh, R. L., and Zak, D. R.: The effects of long term nitrogen deposition on extracellular enzyme activity in an Acer Saccharum forest soil, Soil Biol Biochem., 34(9), 1309-1315, https://doi.org/10.1016/S0038-0717(02)00074-3, 2002.
- Sardans, J., and Peñuelas, J.: Soil Enzyme Activity in a Mediterranean Forest after Six Years of Drought, Soil Sci. Soc. Am. J., 74(3), 838-851, https://doi.org/10.2136/sssaj2009.0225, 2010.
- Schimel, J. P.: Life in Dry Soils: Effects of Drought on Soil Microbial Communities
 and Processes, ANNU REV ECOL EVOL S., 49, 409-432,
 https://doi.org/10.1146/annurev-ecolsys-110617-062614, 2018.
- Schwalm, C. R., Anderegg, W. R. L., Michalak, A. M., Fisher, J. B., Biondi, F., Koch,
 G., Litvak, M., Ogle, K., Shaw, J. D., Wolf, A., Huntzinger, D. N., Schaefer, K.,





- Cook, R., Wei, Y. X., Fang, Y. Y., Hayes, D., Huang, M. Y., Jain, A., and Tian, H.
 Q.: Global patterns of drought recovery, NATURE., 548(7666), 202-205, https://doi.org/10.1038/nature23021, 2017.
- Si, Q., Chen, K., Wei, B., Zhang, Y., Sun, X., and Liang, J.: Formation of particulate organic carbon from dissolved substrate input enhances soil carbon sequestration, EGUsphere., https://doi.org/10.5194/egusphere-2023-1483, 2023.
- Sokol, N. W., Sanderman, J., and Bradford, M. A.: Pathways of mineral-associated soil
 organic matter formation: Integrating the role of plant carbon source, chemistry,
 and point of entry, Glob Chang Biol., 25(1), 12-24, https://doi.org/10.1111/gcb.14482,
 2019.
- Sowerby, A., Emmett, B. A., Williams, D., Beier, C., and Evans, C. D.: The response of dissolved organic carbon (DOC) and the ecosystem carbon balance to experimental drought in a temperate shrubland, Eur. J. Soil Sci.., 61(5), 697-709, https://doi.org/10.1111/j.1365-2389.2010.01276.x, 2010.
- 733 Stursová, M., Zifcáková, L., Leigh, M. B., Burgess, R., and Baldrian, P.: Cellulose 734 utilization in forest litter and soil: identification of bacterial and fungal 735 decomposers, FEMS Microbiol. Ecol.., 80(3), 735-746, 736 https://doi.org/10.1111/j.1574-6941.2012.01343.x, 2012.
- Su, X., Su, X. L., Yang, S. C., Zhou, G. Y., Ni, M. Y., Wang, C., Qin, H., Zhou, X. H.,
 and Deng, J.: Drought changed soil organic carbon composition and bacterial
 carbon metabolizing patterns in a subtropical evergreen forest, Sci. Total Environ.,
 736, https://doi.org/10.1016/j.scitotenv.2020.139568, 2020a.
- Su, X. L., Su, X., Zhou, G. Y., Du, Z. G., Yang, S. C., Ni, M. Y., Qin, H., Huang, Z. Q.,
 Zhou, X. H., and Deng, J.: Drought accelerated recalcitrant carbon loss by
 changing soil aggregation and microbial communities in a subtropical forest, Soil
 Biol Biochem., 148, https://doi.org/10.1016/j.soilbio.2020.107898, 2020b.
- Szejgis, J., Carrillo, Y., Jeffries, T. C., Dijkstra, F. A., Chieppa, J., Horn, S., Bristol, D.,
 Maisnam, P., Eldridge, D., and Nielsen, U. N.: Altered rainfall greatly affects
 enzyme activity but has limited effect on microbial biomass in Australian dryland
 soils, Soil Biol Biochem., 189, https://doi.org/10.1016/j.soilbio.2023.109277, 2024.
- Tiwari, T., Sponseller, R., and Laudon, H.: The emerging role of drought as a regulator
 of dissolved organic carbon in boreal landscapes, Nat. Commun., 13(1),
 https://doi.org/10.1038/s41467-022-32839-3, 2022.
- Tao, F., Houlton, B. Z., Huang, Y. Y., Wang, Y. P., Manzoni, S., Ahrens, B., Mishra, U.,
 Jiang, L. F., Huang, X. M., and Luo, Y. Q.: Convergence in simulating global soil
 organic carbon by structurally different models after data assimilation, Glob
 Chang Biol., 30(5), https://doi.org/10.1111/gcb.17297, 2024.
- Villarino, S. H., Pinto, P., Jackson, R. B., and Piñeiro, G.: Plant rhizodeposition: A key
 factor for soil organic matter formation in stable fractions, Sci Adv., 7(16),
 https://doi.org/10.1126/sciadv.abd3176, 2021.
- Waldrop, M. P., and Firestone, M. K.: Seasonal dynamics of microbial community
 composition and function in oak canopy and open grassland soils, Microb. Ecol.,
 52(3), 470-479, https://doi.org/10.1007/s00248-006-9100-6, 2006.
- Wan, F., Bian, C., Weng, E., Luo, Y., and Xia, J.: TECO-CNP Sv1.0: A coupled carbon-





- nitrogen-phosphorus model with data assimilation for subtropical forests, EGUsphere., https://doi.org/10.5194/egusphere-2025-1243, 2025.
- Wang, X, Zhou, L, Fu, Y, Jiang, Z, Jia, S, Song, B, Liu, D, and Zhou, X.: Drought-induced changes in rare microbial community promoted contribution of microbial necromass C to SOC in a subtropical forest, Soil Biol Biochem., 189, https://doi.org/10.1016/j.soilbio.2023.109252, 2024.
- Willard, S. J., Liang, G. P., Adkins, S., Foley, K., Murray, J., and Waring, B.: Land use
 drives the distribution of free, physically protected, and chemically protected soil
 organic carbon storage at a global scale, Glob Chang Biol., 30(9),
 https://doi.org/10.1111/gcb.17507, 2024.
- Wu, H., Peng, C., Moore, T. R., Hua, D., Li, C., Zhu, Q., Peichl, M., Arain, MA., and
 Guo, Z.: Modeling dissolved organic carbon in temperate forest soils: TRIPLEX DOC model development and validation. Geosci. Model Dev., 7(3), 867-881,
 https://doi.org/10.5194/gmd-7-867-2014, 2014.
- Wu, R. Q., Wang, Y. S., Huo, X. Y., Chen, W. J., and Wang, D. X.: Drought and vegetation restoration patterns shape soil enzyme activity and nutrient limitation dynamics in the loess plateau, J. Environ. Manage., 374. https://doi.org/10.1016/j.jenvman.2024.123846, 2025.
- Wu, J. F., Yao, H. X., Chen, X. H., and Chen, X. W.: Dynamics of dissolved organic
 carbon during drought and flood events: A phase-by-stages perspective, Sci. Total
 Environ., 871, https://doi.org/10.1016/j.scitotenv.2023.162158, 2023.
- Xu, T., White, L., Hui, D. F., and Luo, Y. Q.: Probabilistic inversion of a terrestrial
 ecosystem model: Analysis of uncertainty in parameter estimation and model
 prediction, Global Biogeochem. Cycles., 20(2),
 https://doi.org/10.1029/2005GB002468, 2006.
- Zhao, T. H., Yang, X., He, R., Shi, B. K., Gao, W. F., Ma, J. Y., and Sun, W.: Plant-soil
 microbe adaptive strategies reshape soil respiration components under multi-year
 precipitation frequency reduction and nitrogen addition in a semi-arid grassland,
 Funct. Ecol., 39(9), 2370-2380, https://doi.org/10.1111/1365-2435.70118, 2025.
- Zhou, G. Y., Zhou, X. H., Liu, R. Q., Du, Z. G., Zhou, L. Y., Li, S. S., Liu, H. Y., Shao,
 J. J., Wang, J. W., Nie, Y. Y., Gao, J., Wang, M. H., Zhang, M. Y., Wang, X. H.,
 and Bai, S. H.: Soil fungi and fine root biomass mediate drought-induced
 reductions in soil respiration, Funct. Ecol., 34(12), 2634-2643,
 https://doi.org/10.1111/1365-2435.13677, 2020.
- Zhou, X. Q., Chen, C. R., Wang, Y. F., Xu, Z. H., Duan, J. C., Hao, Y. B., and Smaill,
 S.: Soil extractable carbon and nitrogen, microbial biomass and microbial
 metabolic activity in response to warming and increased precipitation in a semiarid
 Inner Mongolian grassland, GEODERMA., 206, 24-31
 https://doi.org/10.1016/j.geoderma.2013.04.020, 2013.